Lubrication Performance Of Gas-Lubricated Inclined Slider Bearing With Micro-Grooves

Fuxi Liu[1], Wu Guo[1], Yang Li[1], Chunjie Yang[2], Hongbo Kang[2], Zhangyu Chen[1], Guansheng Wu[1], Binhui Han[3], Chaofeng Zhao[4], and Xiang Liu[5*]

[1] 1School of Mechanical and Electrical Engineering, Hunan Applied Technology University, Changde 415100, China
[2] College of Automation, Xi'an University of Posts and Telecommunications, Xi'an 710121, China
[3] School of Automotive Engineering, Xi'an Aeronautical Polytechnic Institute, Xi'an 710089, China
[4] School of Information Technology, Luoyang Normal University, Luoyang 471022, China
[5] Party and Government Office, Hunan Applied Technology University, Changde 415100, China
[*] Corresponding author. E-mail: 1751611391@qq.com

Received: June 08, 2023; Accepted: July 17, 2023

The aim of this paper is to investigate the effect of micro-grooves on the lubrication performance of gas-lubricated inclined slider bearing. This paper is based on numerical analysis. The detailed numerical investigation is carried out in matlab software. The grooving parameters are optimized to obtain the maximum average pressure for various inclination angles of gas-lubricated inclined slider bearing. The results show that the inclination angle of the micro-grooves, depth of the micro-grooves, width of the micro-grooves, and spacing of the micro-grooves have an important influence on the hydrodynamic pressure of gas-lubricated inclined slider bearing with micro-grooves. Besides, the influence of the sliding speed on average pressure increment for various inclination angles of gas-lubricated inclined slider bearing is investigated. It is observed that the sliding speed generating the maximum average pressure increment is dependent on the inclination angle of gas-lubricated inclined slider bearing.

Keywords: Inclined slider bearing; Gas; Micro-grooves; Lubrication performance

http://dx.doi.org/10.6180/jase.202403_27(3).0015

1. Introduction

For improving the performance of bearing, opening micro-grooves in the surface of bearing is an effective way [1–6]. Recently, micro-grooved bearing using an incompressible lubricant attract the attention of researchers. Kumar and Sharma [7] investigated the perfromance of micro-grooved hybrid thrust pad bearing using an incompressible lubricant. They found that opening micro-grooves in the surface of bearing may cause an increase of the bearing stiffness coefficient and bearing load-carrying capacity. They also found that opening micro-grooves in the surface of bearing may cause a reduction of the frictional power loss. Bhardwaj et al. [8] studied the performance of micro-grooved thrust ball bearing using an incompressible lubricant. The experimental results showed that micro-grooves could reduce the vibration and frictional torque. Feng et al. [9] studied the performance of micro-grooved journal bearing using an incompressible lubricant. They found that the use of micro-grooves could increase the bearing load-carrying capacity at the smaller eccentricity ratio. Sharma and Tomar [10] studied the performance of micro-grooved spherical journal bearing using an incompressible lubricant. Their results showed that using the micro-grooves and magneto-rheological fluid could improve the bearing stability. Han and Fu [11] studied the lubrication performance of micro-grooved misaligned bearing using an incompressible lubricant. It was shown that the lubrication

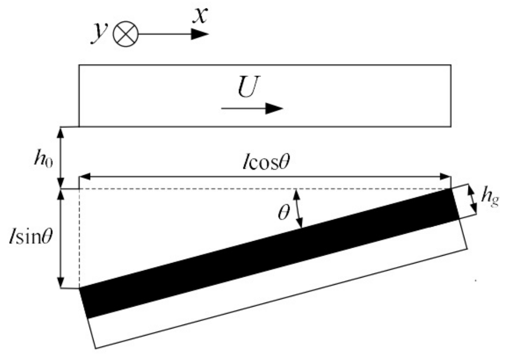

Fig. 1. Model of gas-lubricated inclined slider bearing with micro-grooves

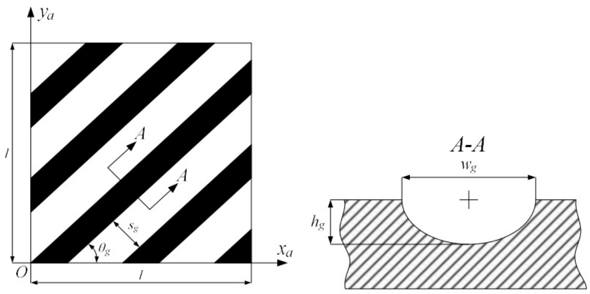

Fig. 2. Model of the lower slider [14].

performance of bearing depends on the micro-groove position. Fu et al. [12] studied the lubrication performance of parallel slider bearing using an incompressible lubricant. It was found that the lubrication performance of bearing could be improved by using short grooves.

Micro-grooved bearing using a compressible lubricant also attract the attention of researchers. LaTray and Kim [13] studied the performance of micro-grooved thrust foil bearing. Their results showed that adding the micro-grooves on the top foil could reduce the bearing power loss. Yu et al. [14] studied the performance of micro-grooved gas-lubricated thrust bearing by using the chaos-enhanced accelerated particle swarm algorithm. It was shown that a higher load-carrying capacity could be obtained by adopting discontinuous micro-grooves.Liu et al. [15] studied the influence of parabolic grooves on the load-carrying capacity of three-pad fixing-pad aerodynamic journal bearing. It was shown that the bearing load-carrying capacity could be improved by using parabolic grooves. Feng et al. [16] investigated the performance of gas foil journal bearing with taper-grooves. They found that the bearing static property and bearing dynamic property could be improved by using taper-grooves.

The lubrication performance of gas-lubricated parallel bearing with micro-grooves have been systematically investigated [17]. However, the lubrication performance of gas-lubricated inclined bearing with micro-grooves is not investigated. The present study is intended to investigate the lubrication performance of gas-lubricated inclined bearing with micro-grooves.

2. The model

The model of gas-lubricated inclined slider bearing with micro-grooves is shown in Fig. 1. The speed of the upper slider is U. The lubricant of gas-lubricated inclined slider bearing with micro-grooves is an ideal gas. The lower slider is fixed and the micro-grooves are evenly distributed in the lower slider. The minimum clearance of gas-lubricated inclined slider bearing with micro-grooves is h_0. The inclination angle of gas-lubricated inclined slider bearing with micro-grooves is θ, l is the lower slider length. h_g is the micro-groove depth.

Fig. 2 presents the model of the lower slider. θ_g is the micro-groove inclination angle. s_g is the micro-groove spacing. w_g is the micro-groove width.

The relation between the xOy coordinate system and x_aOy_a coordinate system is shown in Fig. 3 The angle between the x axis and x_a axis is θ. The direction of the y axis is the same as the direction of the y_a axis.

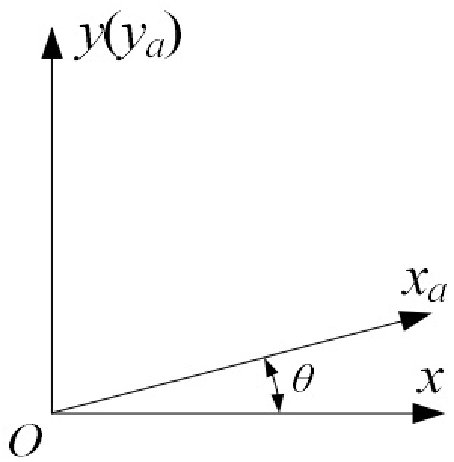

Fig. 3. Relation between the xOy coordinate system and x_aOy_a coordinate system

In the steady-state condition, the Reynolds equation is described as:

$$\frac{\partial}{\partial x}\left(ph^3\frac{\partial p}{\partial x}\right)+\frac{\partial}{\partial y}\left(ph^3\frac{\partial p}{\partial y}\right)=6\mu U\frac{\partial(ph)}{\partial x} \quad (1)$$

where h is the bearing clearance, p is the bearing pressure, μ is the bearing viscosity.

The dimensionless variables are obtained by:

$$X = x/w_0, Y = y/w_0, P = p/p_a, H = h/h_0 \tag{2}$$

where w_0 is the reference value, p_a is the ambient pressure.

In the steady-state condition, the dimensionless Reynolds equation is described as:

$$\frac{\partial}{\partial X}\left(PH^3\frac{\partial P}{\partial X}\right) + \frac{\partial}{\partial Y}\left(PH^3\frac{\partial P}{\partial Y}\right) = \Lambda\frac{\partial(PH)}{\partial X} \tag{3}$$

where $\Lambda = 6\mu U w_0/\left(p_a h_0^2\right)$.

The dimensionless thickness H is described as:

case 1: $0^\circ \le \theta_g < 90^\circ$

$$H = \begin{cases} 1 + \dfrac{(L\cos\theta - X)w_0\tan\theta}{h_0} + H_g - \\ \dfrac{4H_g}{W_g^2}\left[\left(\dfrac{X\tan\theta_g}{\cos\theta} - Y\right)\cos\theta_g - n_1 L_g - \dfrac{1}{2}W_g\right]^2, \\ \quad Y < \dfrac{X\tan\theta_g}{\cos\theta} \text{ and } Y_1 < Y < Y_2 \\ 1 + \dfrac{(L\cos\theta - X)w_0\tan\theta}{h_0} + H_g - \\ \dfrac{4H_g}{W_g^2}\left[\left(Y - \dfrac{X\tan\theta_g}{\cos\theta}\right)\cos\theta_g - n_1 L_g - \dfrac{1}{2}W_g\right]^2, \\ \quad Y > \dfrac{X\tan\theta_g}{\cos\theta} \text{ and } Y_3 < Y < Y_4 \\ 1, \quad \text{elsewhere} \end{cases} \tag{4}$$

case 2: $\theta_g = 90^\circ$

$$H = \begin{cases} 1 + \dfrac{(L\cos\theta - X)w_0\tan\theta}{h_0} + H_g \\ \dfrac{4H_g}{W_g^2}\left(\dfrac{X}{\cos\theta} - n_2 L_g - \dfrac{1}{2}W_g\right)^2, \\ X > n_2 L_g\cos\theta \text{ and } X < \left(n_2 L_g + W_g\right)\cos\theta \\ 1, \quad \text{elsewhere} \end{cases} \tag{5}$$

where

$$\left.\begin{aligned} Y_1 &= \tfrac{X\tan\theta_g}{\cos\theta} - \left(n_1 L_g + W_g\right)\sec\theta_g \\ Y_2 &= \tfrac{X\tan\theta_g}{\cos\theta} - n_1 L_g\sec\theta_g \\ Y_3 &= \tfrac{X\tan\theta_g}{\cos\theta} + \left(n_1 L_g + S_g\right)\sec\theta_g \\ Y_4 &= \tfrac{X\tan\theta_g}{\cos\theta} + \left(n_1 + 1\right) L_g\sec\theta_g \end{aligned}\right\} \tag{6}$$

$$L_g = \left(w_g + s_g\right)/w_0 \tag{7}$$

$$n_1 = fix\left|\left(\frac{X\sin\theta_g}{\cos\theta} - Y\cos\theta_g\right)/L_g\right| \tag{8}$$

$$n_2 = fix\left|\frac{X}{L_g\cos\theta}\right| \tag{9}$$

fix is a rounding function, $H_g = h_g/h_0$ is the dimensionless depth, $S_g = s_g/w_0$ is the dimensionless spacing, $W_g = w_g/w_0$ is the dimensionless width, $L = l/w_0$ is the dimensionless length.

The boundary conditions of the micro-groove list is described as:

$$P(0,Y) = P(L\cos\theta, Y) = P(X,0) = P(X,L) = 1 \tag{10}$$

Eq. (3) is solved by adopting the multi-grid finite element method [18]. After Eq. (3) is solved, the dimensionless average pressure P_{av} is calculated by:

$$P_{av} = \frac{p_{av}}{p_a} = \frac{\int_0^L \int_0^{L\cos\theta} PdXdY}{L^2\cos\theta} \tag{11}$$

The average pressure increment P_i is calculated by:

$$P_i = \frac{P_{av} - P_s}{P_s} \tag{12}$$

where P_{av} is the dimensionless average pressure of gas-lubricated inclined slider bearing with micro-grooves, P_s is the dimensionless average pressure of smooth gas-lubricated inclined slider bearing.

3. Result and discussions

When the lubrication performance of gas-lubricated inclined slider bearing with micro-grooves is investigated, some calculation parameters are constant. The constant are as follows: $p_a = 0.101325\text{MPa}, c = 2.5\times10^{-4}$ mm, $\mu = 1.8\times10^{-5}$ Pa · s, $w_0 = 0.05$ mm, and $l = 2.5$ mm.

Fig. 4 displays the pressure distribution of smooth gas-lubricated inclined slider bearing. Fig. 5 displays the pressure distribution of $\theta_g = 90^\circ$. It is noted that the maximum pressure of $\theta_g = 90^\circ$ is greater than that of smooth gas-lubricated inclined slider bearing. It is also noted that the minimum pressure of $\theta_g = 90^\circ$ is less than that of smooth gas-lubricated inclined slider bearing. These results indicate that opening micro-grooves could change the pressure distribution of gas-lubricated inclined slider bearing.

Fig. 6 displays the influence of the inclination angle of the micro-grooves on average pressure increment for various inclination angles of gas-lubricated inclined slider bearing. It is noted that there is an optimum micro-groove inclination angle for maximizing the hydrodynamic pressure. When $\theta = 20\mu$rad, the optimum micro-groove inclination angle is 90°. When $\theta = 40\mu$rad, the optimum micro-groove inclination angle is 90°. When $\theta = 60\mu$rad, the optimum micro-groove inclination angle is 90°. These

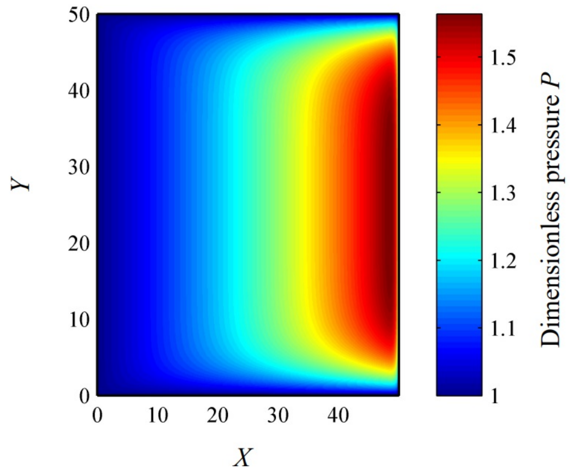

Fig. 4. Dimensionless pressure distribution of smooth gas-lubricated inclined slider bearing ($\theta = 60\,\mu$rad and $U = 5\,\mathrm{m/s}$)

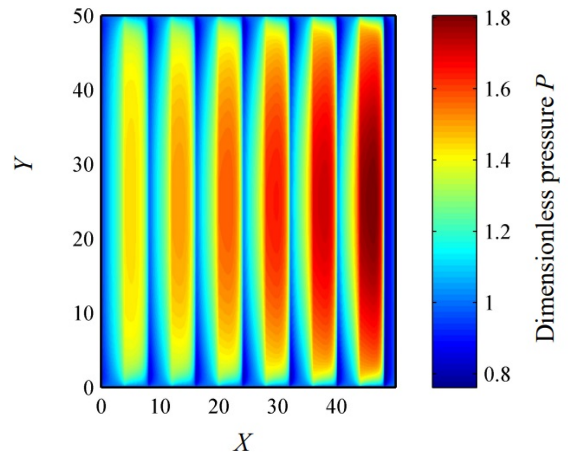

Fig. 5. Dimensionless pressure distribution of $\theta_g = 90°(\theta = 60\,\mu\mathrm{rad}, U = 5\,\mathrm{m/s}, H_g = 4, W_g = 4$, and $S_g = 4)$

results indicate that the micro-grooves perpendicular to the direction of the movement could generate the maximum hydrodynamic pressure. The result is in agreement with that obtained by Lu et al. [17].

Fig. 7 displays the influence of the micro-groove depth on average pressure increment for various inclination angles of gas-lubricated inclined slider bearing. When $\theta = 20\mu$rad, the dimensionless micro-groove depth generating the maximum hydrodynamic pressure is 3 . When $\theta = 40\mu$rad, the dimensionless micro-grooves depth generating the maximum hydrodynamic pressure is 3 . When $\theta = 60\mu$rad, the dimensionless micro-groove depth generating the maximum hydrodynamic pressure is 2 . These

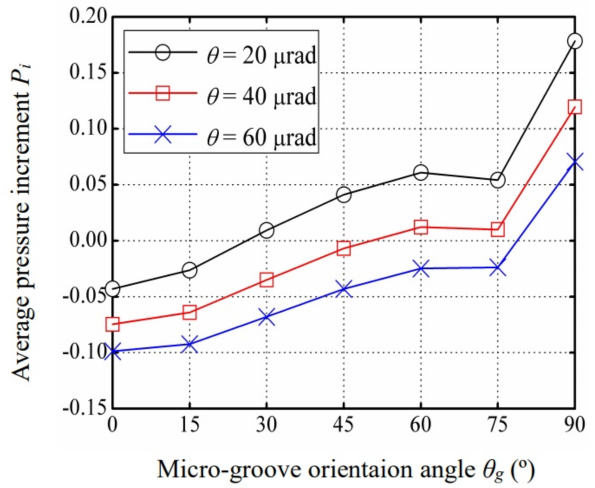

Fig. 6. Influence of the inclination angle of the micro-grooves on average pressure increment for various inclination angles of gas-lubricated inclined slider bearing $(U = 5\,\mathrm{m/s}, H_g = 4, W_g = 4$, and $S_g = 4)$

results show that when the maximum hydrodynamic pressure is obtained, the micro-grooves should be properly fabricated, neither too deep nor too shallow. The result is in agreement with that obtained by Lu et al. [17]. These results also show that the micro-groove depth maximizing the hydrodynamic pressure is dependent on the inclination angle of gas-lubricated inclined slider bearing.

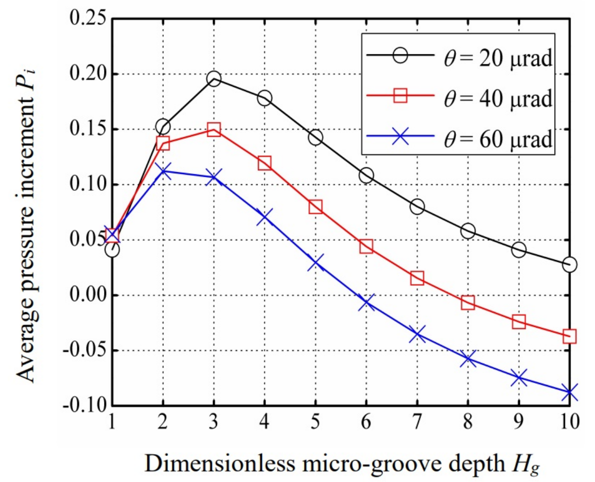

Fig. 7. Influence of the micro-groove depth on average pressure increment for various inclination angles of gas-lubricated inclined slider bearing $(U = 5\,\mathrm{m/s}, \theta_g = 90°\ \ W_g = 4$, and $S_g = 4)$

Fig. 8 displays the effect of the micro-groove width on average pressure increment for various inclination angles of gas-lubricated inclined slider bearing. It is observed that both too wide micro-grooves and too narrow micro-grooves could not obtain the maximum average pressure. Therefore, a proper micro-groove width should be chosen for maximizing the hydrodynamic pressure. It is also observed that the micro-groove width maximizing the hydrodynamic pressure is dependent on the inclination angle of gas-lubricated inclined slider bearing.

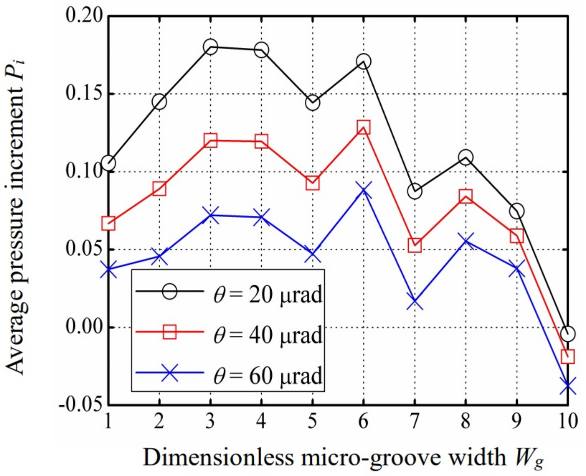

Fig. 8. Effect of the micro-groove width on average pressure increment for various inclination angles of gas-lubricated inclined slider bearing $(U = 5\,\mathrm{m/s}, \theta_g = 90^\circ\ H_g = 4, \text{and } S_g = 4)$

Fig. 9 displays the effect of the micro-groove spacing on average pressure increment for various inclination angles of gas-lubricated inclined slider bearing. When $\theta = 20\mu$rad, the dimensionless micro-groove spacing maximizing the hydrodynamic pressure is 46 . When $\theta = 40\mu$rad, the dimensionless micro-groove spacing maximizing the hydrodynamic pressure is 46 . When $\theta = 60\mu$rad, the dimensionless micro-groove spacing maximizing the hydrodynamic pressure is 46 . These results are in agreement with those obtained by Lu et al. [17]. These results also show that the micro-groove spacing maximizing the hydrodynamic pressure is independent on the inclination angle of gas-lubricated inclined slider bearing.

Fig. 10 presents the influence of the sliding speed on average pressure increment for various inclination angles of gas-lubricated inclined slider bearing. It is observed that opening micro-grooves could increase the average pressure of gas-lubricated inclined slider bearing for any given sliding speed. It is also observed that the average pressure increment first increases and then decreases with increasing the sliding speed. This result indicates that an optimum sliding speed should be chosen in order to maximizing

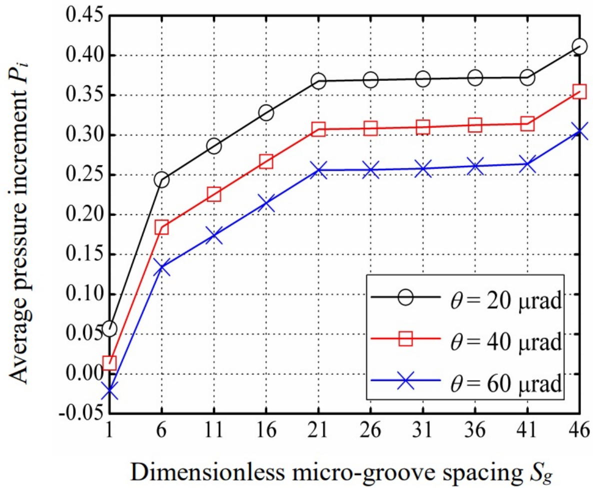

Fig. 9. Effect of the micro-groove spacing on average pressure increment for various inclination angles of gas-lubricated inclined slider bearing $(U = 5\,\mathrm{m/s}, \theta_g = 90^\circ\ H_g = 4, \text{and } W_g = 4)$

the average pressure increment. When $\theta = 20\mu$rad, the optimum sliding speed is 8 m/s. When $\theta = 40\mu$rad, the optimum sliding speed is 9 m/s. When $\theta = 60\mu$rad, the optimum sliding speed is 11 m/s. This result implies that the optimum sliding speed is dependent on the inclination angle of gas-lubricated inclined slider bearing.

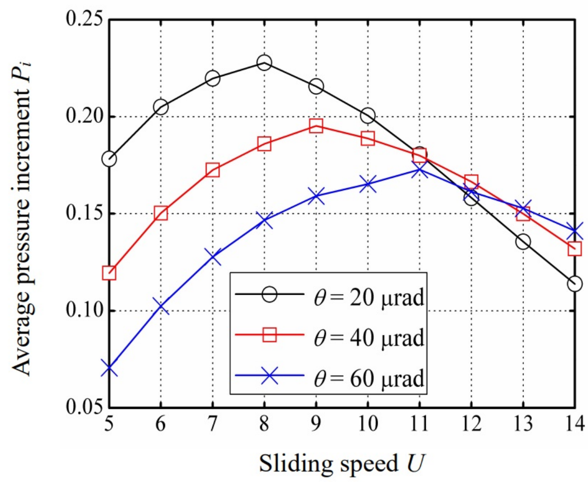

Fig. 10. Influence of sliding speed on average pressure increment for various inclination angles of gas-lubricated inclined slider bearing $(\theta_g = 90^\circ, H_g = 4, W_g = 4 \text{ and } S_g = 4)$

4. Conclusions

The lubrication performance of gas-lubricated inclined slider bearing with micro-grooves is investigated in the present study. The following conclusions are obtained:

1. The hydrodynamic pressure is controlled by the inclination angel of the micro-grooves. The micro-grooves perpendicular to the direction of the movement could maximize the hydrodynamic pressure.

2. The depth of the micro-grooves maximizing the hydrodynamic pressure is dependent on the inclination angle of gas-lubricated inclined slider bearing.

3. The width of the micro-grooves maximizing the hydrodynamic pressure is dependent on the inclination angle of gas-lubricated inclined slider bearing.

4. The spacing of the micro-grooves maximizing the hydrodynamic pressure is independent on the inclination angle of gas-lubricated inclined slider bearing.

5. The sliding speed maximizing the hydrodynamic pressure is dependent on the inclination angle of gas-lubricated inclined slider bearing.

The results of this study is beneficial for designing micro-grooved gas-lubricated inclined slider bearing. In this paper, the influence of the geometrical shape of micro-grooves on the lubrication performance of gas-lubricated inclined bearing with micro-grooves is not studied. In future work, we will investigate the effect of the geometrical shape of micro-grooves on the lubrication performance of gas-lubricated inclined bearing with micro-grooves.

Acknowledgements

This study was supported by the Teaching Research Reform Project of Hunan Applied Technology University in 2022 (No. 4), Funding Scheme of Key Scientific Research of Henan's Higher Education Institutions (No. 22A120009), and Henan Provincial Department of Science and Technology key R&D and Promotion Special Project (No. 222102210104).

References

[1] M. Scaraggi, (2014) *"Optimal textures for increasing the load support in a thrust bearing pad geometry"* **Tribology Letters** ***53***(1): 127–143.

[2] V. Kumar, S. C. Sharma, and K. Narwat, (2020) *"Influence of micro-groove attributes on frictional power loss and load-carrying capacity of hybrid thrust bearing"* **Industrial Lubrication and Tribology** ***72***(5): 589–598.

[3] B. Jalilia, A. Mousavia, P. Jalili, A. Shateria, and D. Domiri Ganji, (2022) *"Thermal analysis of fluid flow with heat generation for different logarithmic surfaces"* **International Journal of Engineering, Transactions B: Applications** ***35***(12): 2291–2296.

[4] E. Eswanto, H. Hasan, and Z. M. Razlan, (2023) *"An analysis on performance of pico-hydro with archimedes screw model viewed from turbine shaft angle"* **International Journal of Engineering, Transactions A: Basics** ***36***(1): 10–18.

[5] A. Karbasian, M. Shirazi, and A. H. Mahmoudi, (2023) *"Effect of surface roughness on brinell hardness and load-displacement curves using a macro indentation"* **International Journal of Engineering, Transactions B: Applications** ***36***(5): 914–924.

[6] N. Agrawal and S. C. Sharma, (2023) *"Micro-grooved hybrid spherical thrust bearing with Non-Newtonian lubricant behaviour"* **International Journal of Mechanical Sciences** ***240***: 107940.

[7] V. Kumar and S. C. Sharma, (2019) *"Effect of geometric shape of micro-grooves on the performance of textured hybrid thrust pad bearing"* **Journal of the Brazilian Society of Mechanical Sciences and Engineering** ***41***(11): 508.

[8] V. Bhardwaj, R. K. Pandey, and V. K. Agarwa, (2021) *"Experimental exploration for the performance improvement of a thrust ball bearing using circumferential micro-grooved races"* **Surface Topography: Metrology and Properties** ***9***(3): 035017.

[9] H. H. Feng, S. Y. Jiang, and Y. Q. Shang-Guan, (2021) *"Three-dimensional computational fluid dynamic analysis of high-speed water-lubricated hydrodynamic journal bearing with groove texture considering turbulence"* **Proceedings of the Institution of Mechanical Engineers, Part J: Journal of Engineering Tribology** ***235***(11): 2272–2286.

[10] S. C. Sharma and A. K. Tomar, (2021) *"Study on MR fluid hybrid hole-entry spherical journal bearing with micro-grooves"* **International Journal of Mechanical Sciences** ***202-203***: 106504.

[11] Y. X. Han and Y. H. Fu, (2020) *"Influence of micro-grooves on the lubrication performance of a misaligned bearing"* **Proceedings of the Institution of Mechanical Engineers, Part J: Journal of Engineering Tribology** ***234***(6): 887–889.

[12] H. Fu, Y. H. Fu, J. H. Ji, S. C. Zhao, and X. J. Hua, (2018) *"Influence of short grooves on hydrodynamic lubrication of textured infinitely long sliders"* **Advances in Mechanical Engineering *10***(2):

[13] N. LaTray and D. Kim, (2021) *"Novel thrust foil bearing with pocket grooves for enhanced static performance"* **Journal of Tribology *143***(11): 111803.

[14] Y. L. Yu, G. Pu, T. C. Jiang, and K. Jiang, (2020) *"Discontinuous grooves in thrust air bearings designed with CAPSO algorithm"* **International Journal of Mechanical Sciences *165***: 105197.

[15] F. X. Liu, Y. J. Lu, Q. M. Zhang, Y. F. Zhang, P. Gupta, and N. Müller, (2016) *"Load performance analysis of three-pad fixing pad aerodynamic journal bearings with parabolic grooves"* **Lubrication Science *28***(4): 207–220.

[16] M. Feng, H. Y. Hu, and T. M. Ren, (2020) *"Performance potential of gas foil journal bearings enhanced with micro taper-grooves on top foil"* **Industrial Lubrication and Tribology *72***(3): 299–306.

[17] Y. J. Lu, F. X. Liu, and Y. F. Zhang, (2017) *"Hydrodynamic lubrication of micro-grooved gas parallel slider bearings with parabolic grooves"* **Mechanika *23***(6): 931–936.

[18] F. X. Liu, Z. L. Li, C. J. Yang, H. B. Wu, H. Z. Yin, and S. Jiang, (2021) *"Hydrodynamic lubrication of partially textured gas parallel slider bearings with orientation ellipse dimples"* **Mathematical Problems in Engineering *2021***: 4441892.